Thermochimica Acta, 228 (1993) 173–189
Elsevier Science Publishers B.V., Amsterdam

Spectroscopic and microscopic investigations of the thermal decomposition of nickel oxysalts. Part 2. Nickel nitrate hexahydrate

Seham A.A. Mansour

Chemistry Department, Faculty of Science, Minia University, El-Minia (Egypt)

(Received 23 February 1993; accepted 20 March 1993)

Abstract

The thermal decomposition of nickel nitrate hexahydrate (NiNHH) under dynamic atmosphere of air has been thoroughly studied. Reactions occurring throughout the decomposition up to 600°C were monitored by means of thermogravimetry (TG) and differential thermal analysis (DTA). These reactions were characterized by analysis of the solid calcination products at different temperatures at which various intermediates were expected. Solid analysis was carried out using infrared spectroscopy and X-ray diffractometry. Non-isothermal kinetic parameters (ΔE, A and k) were determined. TG and DTA under nitrogen atmosphere has been carried out. The results indicate the formation of $Ni(NO_3)_2 \cdot nH_2O$ (where $n = 5.5$, 4 and 2) and mixture of anhydrous and basic nickel nitrate as intermediate solid products. Basic nickel nitrate intermediate was formed in nitrogen atmosphere as well as in air, which was attributed to a hydrolysis process involving the water of dihydrate intermediate. The morphological changes throughout the decomposition course have been followed by scanning electron microscopy and the results are correlated with the obtained thermoanalytical results of the decomposition course of NiNHH.

INTRODUCTION

The thermal decomposition of common metal nitrates is an important class of reactions in the chemical industry. It has applications in the preparation of high surface area materials for catalysts, molecular sieves, and adsorbents as well as being of interest for ecological and environmental reasons [1, 2].

In 1985, Dollimore et al. [3] surveyed previous studies on the thermal behaviour of nickel nitrate hexahydrate, and concluded that many reports were conflicting in their description of the observed intermediates. They explained some of these reported conflict in terms of experimental conditions. Later on, the same investigators [4] suggested a mechanism of degradation of the nickel nitrate hexahydrate from an EGA study. They reported that the degradation processes was dominated by the coordination chemistry of nickel, the rate of water removal from the sample and the

ability of water vapour to hydrolyse the intermediate nickel dinitrate. They suggested that nickel nitrate decomposition occurred either as a single step

$$Ni(NO_3)_2 \rightarrow NiO + N_2O_5$$

or as two steps

$$Ni(NO_3)_2 \rightarrow Ni(NO_2)_2 + O_2$$

$$Ni(NO_2)_2 \rightarrow NiO + N_2O_3$$

However, the decomposition of nickel nitrate has been claimed [5] to take place in a single step, according to the equation

$$Ni(NO_3)_2 \rightarrow NiO + 2NO_2 + \tfrac{1}{2}O_2$$

The prupose of this study is to obtain a more comprehensive physiochemical understanding of the course of the decomposition of nickel nitrate hexahydrate. The study includes thermal analyses via differential thermal analysis (DTA) and thermogravimetric analysis (TGA), in order to elucidate the decomposition pathways. Supplementary analytical methods have been adopted namely infrared spectroscopy, X-ray diffractometry (XRD) and scanning electron microscopy (SEM) to determine the structure of the intermediates and the final decomposition products.

EXPERIMENTAL

Materials

Nickel nitrate hexahydrate $Ni(NO_3)_2 \cdot 6H_2O$ (NiNHH) used was 99.9% pure, BDH (UK). In view of the thermal analyses results (vide infra), decomposition solid products were obtained by calcination of (NiNHH) at various temperatures for 2 h, in a still atmosphere of air, and then kept dry for further study.

Thermal analysis

TG and DT analyses of NiNHH were performed by heating at various rates ($\theta = 2, 5, 10, 20\,K\,min^{-1}$) to 600°C in a dynamic atmosphere of air ($30\,cm^3\,min^{-1}$). Further TG and DTA runs were carried out under dynamic atmosphere of nitrogen ($30\,cm^3\,min^{-1}$) at a heating rate of $10\,K\,min^{-1}$. An automatically recording Shimadzu Unit (Model 30H; Kyoto, Japan) was used in performing these analyses. Sample size was constant for all runs ($\approx$10 mg) and highly sintered α-Al_2O_3 was the reference material for the DTA measurements.

Infrared spectroscopy

Infrared analysis of NiNHH and its calcination solid products was carried out over the frequency range 4000–300 cm^{-1}, with a resolution of 5.3 cm^{-1} by means of a Model 580B Perkin–Elmer spectrophotometer (UK). IR

Spectra were measured on thin (<20 mg cm^{-2}), lightly loaded (<1%) KBr discs.

X-ray diffractometry

XRD analysis of NiNHH and its calcination products was carried out using a Model JSX-60 PA Jeol diffractometer (Japan), using Ni-filtered Cu Kα radiation. For identification purposes, the diffraction patterns (I/I_0 versus d-spacing) were matched with relevant ASTM standards.

Kinetic analysis procedure of thermoanalytical data

From the measured thermoanalytical curves, the temperature (T_{max}) at which the sample decomposes to the same extent (where the weight loss processes are maximized), or corresponding to the peaks of the DTA curves (corresponding to weight-invarient processes), was determined as a function of the heating rate.

The activation energy ΔE (kJ mol^{-1}) was then calculated for each process from plots of log θ against $(1/T_{max})$ according to the relationship [6]

$$\Delta E = 2.19R \, \mathrm{d} \log \theta / \mathrm{d}(1/T_{max}) \quad (1)$$

where R is the gas constant (8.314 J mol^{-1} K^{-1}).

Calculation of the frequency factor A (min^{-1}) for the weight loss processes was carried out, assuming first-order kinetics, using the equation [7]

$$\log[-\log(1-C)/T_{max}^2] = \log AR/\theta\Delta E - \Delta E/2.3RT_{max} \quad (2)$$

where C is the fractional extent decomposed.

The rate constant k (min^{-1}) is then obtained from the Arrhenius equation

$$k = A \exp(-\Delta E/RT) \quad (3)$$

Electron microscopy

Samples of NiNHH and its calcination products were examined using a Jeol scanning electron microscope, model 35CF. The samples were mounted separately on aluminium stubs by clear adhesive and precoated with gold/palladium in a sputter-coater to minimize the charging effect of the materials. For each sample, many crystals were exmained and only features identified as being typical, reproducible and significant were photographed.

RESULTS AND DISCUSSION

Thermal events encountered in the course of nickel nitrate hexahydrate decomposition

The TG and DTA curves for nickel nitrate hexahydrate (NiNHH), under dynamic atmosphere of air and heating rates of 2, 5, 10 and

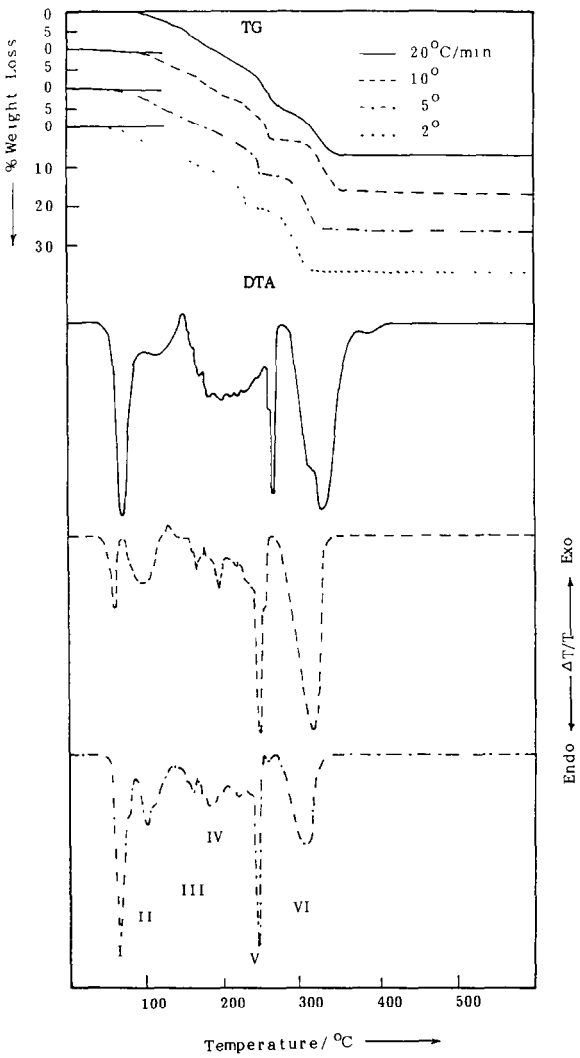

Fig. 1. TG and DTA curves of NiNHH, in a dynamic atmosphere of air (30 cm^3 min^{-1}), at the heating rates indicated. Roman numerals I–VI indicate locations of the stages of decomposition.

20 K min^{-1} are shown in Fig. 1. TG curves indicate that the parent material suffers about 42% loss of its original weight before reaching a thermally stable intermediate. The TG curves also show more than one break in its weight loss. However the DTA curves indicate that the weight loss involves five endothermic processes. Further weight loss occurs with an endothermic process, bringing the total weight loss of the original material up to 74%, which is very close to the calculated value (74.3%) for $NiNO_3 \cdot 6H_2O \rightarrow NiO$ transformation. For simplicity, these stages are referred to as I, II, III, IV, V and VI. It is to be noted that, these stages are more pronounced in the DTA curve than the corresponding TG (Fig. 1). The characteristic features of these stages are listed in Table 1. For

TABLE 1

Relationship between the heating rate θ (in K min^{-1}) and the peak temperature T_{max} (in °C) in the DTA curves corresponding to the various endothermic stages (I–VI) in the decomposition of NiNHH

Stage	T_{max}				Weight loss [a]
	$\theta = 2$	$\theta = 5$	$\theta = 10$	$\theta = 20$	
I	55	60	65	75	Melting
II	85	90	95	110	3
III	155	160	165	180	12.3
IV	170	180	195	200	24.4
V	238	245	250	270	45
VI	300	305	315	330	72.5

[a] Percent.

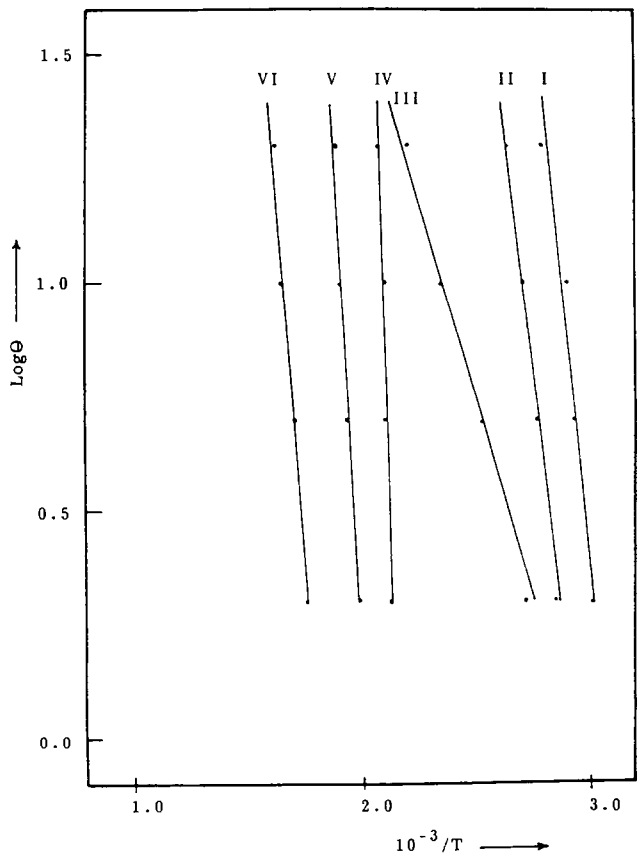

Fig. 2. Plots of log θ vs. $1/T$ for NiNHH decomposition stages (from the DTA curves shown in Fig. 1).

TABLE 2

Non-isothermal kinetic parameters[a] of the various stages in the decomposition of NiNHH from TG and DTA

Parameter	Stage					
	I	II	III	IV	V	VI
ΔE	79	72.0	36	130	140	96
$k \times 10^{-2}$		1.69	4.2	10.2	13	6.2
$\log A$	10.12	10.03	10.05	10.1	10.08	10.03

[a] ΔE in kJ mol^{-1}; k in min^{-1}.

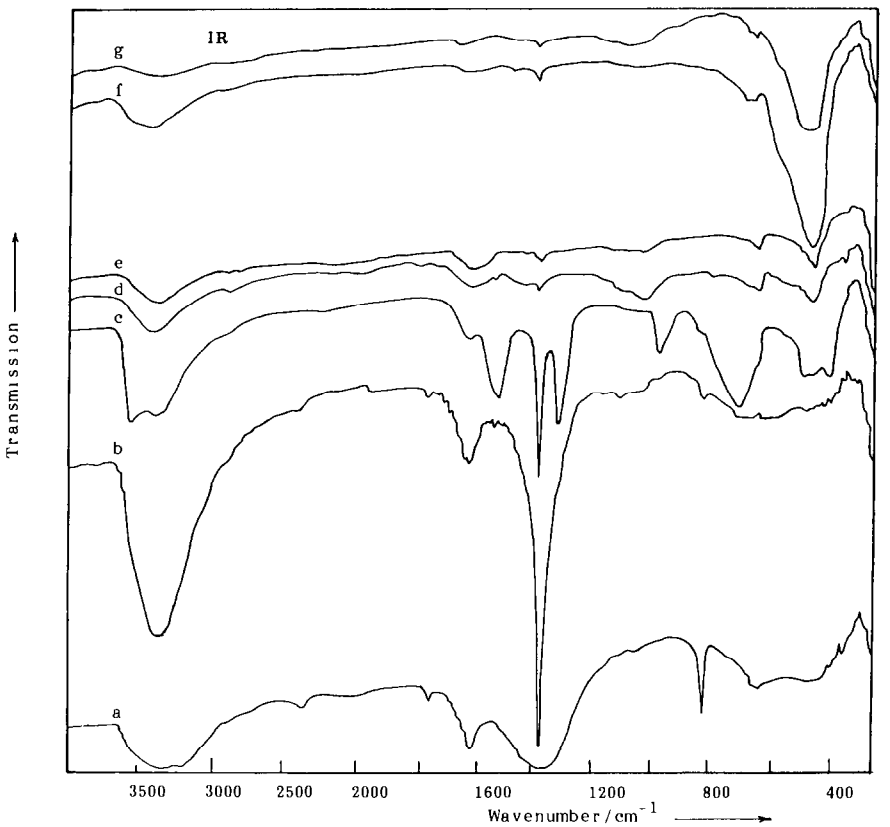

Fig. 3. IR spectra of NiNHH (curve a) and its solid calcination products at 150°C (curve b), 220°C (curve c), 270°C (curve d), 350°C (curve e), 400°C (curve f) and 600°C (curve g).

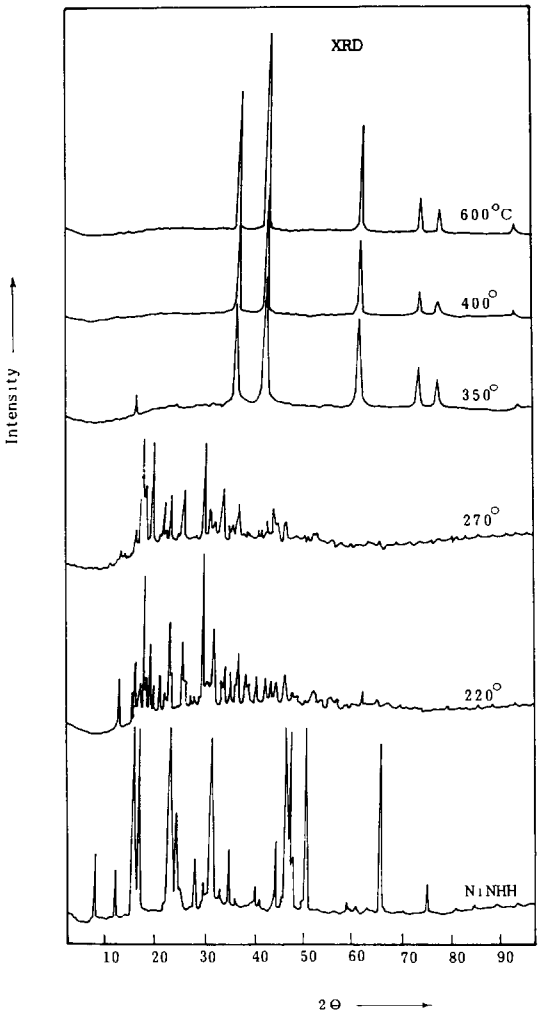

Fig. 4. X-Ray powder diffractograms of NiNHH and its solid decomposition products obtained after calcination for 2 h at the temperatures indicated.

convenience, the discussion of the thermal behavior of NiNHH will be based on the TG and DTA obtained at heating rate of 10 K min^{-1}.

Log θ versus $1/T$ plots (Fig. 2) from TG and DTA results were used to calculate the non-isothermal kinetic parameters ΔE, k and log A, which are compiled in Table 2.

Figure 3 and 4 show respectively IR spectra and X-ray diffractograms of NiNHH and its solid calcination products from 65 to 600°C, in air.

Figure 5 shows the TG and DTA curves obtained under dynamic nitrogen atmosphere (30 ml min^{-1}) at heating rate of 10 K min^{-1}.

Characterization of the thermal events

Stages I and II

DTA and TG curves (Fig. 1) show that the endothermic event I is sharp (DTA) and a weight invariant process. This event could be attributed to melting of NiNHH. The endothermic event II (Fig. 1) was found to correspond to a weight loss of 3% equal to the calculated value for the loss of 0.5 mol of water per mole of NiNHH. According to Dollimore et al. [3], the formation of the intermediate of composition $Ni(NO_3)_2 \cdot 5\frac{1}{2}H_2O$ could be achieved through the ability of water to act both as a unidentate ligand and as a bridging ligand, which in turn helps nickel to maintain an octahedral field. The activation energies of these two events were 79 and 72 kJ mol^{-1} respectively. Such high values indicate that they involve further structural rearrangements accompanying the release of water. Thus

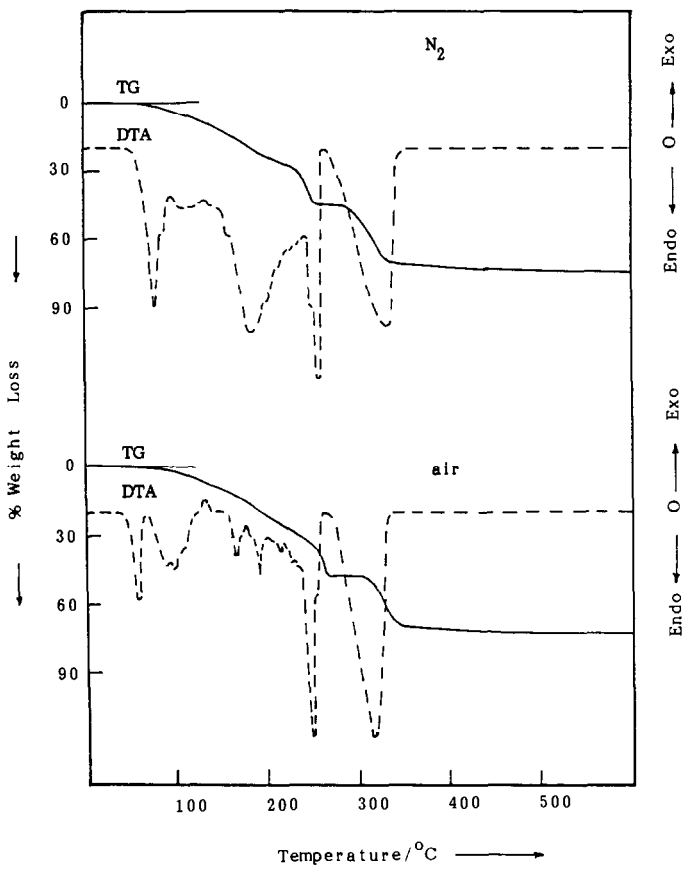

Fig. 5. TG and DTA curves recorded at 10 K min^{-1} for NiNHH in dynamic atmospheres (30 cm^3 min^{-1}) of air and nitrogen.

the dehydration can occur as follows

$$Ni(NO_3)_2 \cdot 6H_2O \xrightarrow[\text{rearrangement}]{\text{structural}}$$

$$Ni(H_2O)_6(NO_3)_2 \xrightarrow{-0.5H_2O} \tfrac{1}{2}[Ni_2(H_2O)_{11}(NO_3)_4]$$

Stage III

Heating NiNHH up to 150°C resulted in a further loss of 13% of its original weight (Fig. 1). This is close to that anticipated for the dehydration process $Ni(NO_3)_2 \cdot 6H_2O \rightarrow Ni(NO_3)_2 \cdot 4H_2O$.

The IR spectrum of the calcination product obtained at 150°C (Fig. 3 curve b) is quite similar to that obtained from untreated NiNHH (Fig. 3 curve a) in that there are characteristic absorptions of nitrate ions (1380 and 823 cm^{-1}) [8]. The spectrum (Fig. 3, curve b) shows absorption bands at 1035, 1460, 1310 and 745 cm^{-1} which can be assigned to nickel nitrate tetrahydrate $Ni(NO_3)_2 \cdot 4H_2O$. Furthermore XRD analysis (Fig. 4) of the calcination product at 150°C shows the lines characteristic of $Ni(NO_3)_2 \cdot 4H_2O$ (ASTM card no. 22-751).

The calculated activation energy for event III (Table 1) amounts to 36 kJ mol^{-1}. Such a low value compared to those for the preceding stages may suggest that the H_2O released has been driven off from weak leakages formed from the earlier release of $0.5H_2O$. Hence, stage III obviously accounts for the formation of nickel nitrate tetrahydrate intermediate as follows

$$0.5[Ni_2(H_2O)_{11}(NO_3)_4] \xrightarrow{-1.5H_2O} Ni(NO_3)_2 \cdot 4H_2O$$

Stage IV

The DTA curve (Fig. 1) (at 10 K min^{-1}) shows that stage IV takes place endothermically in the temperature range 175–220°C with a maximum at 195°C. The corresponding TG curve (Fig. 1) reveals that the total weight loss up to 220°C amounts to 27% which is slightly higher than the calculated value for nickel nitrate hexahydrate → nickel nitrate dihydrate transformation. However, the IR spectrum of the calcination product obtained at 220°C (Fig. 3, curve c) displays absorptions at 1530 and 1310 cm^{-1}. These are assigned to nickel nitrate dihydrate in addition to the absorptions of the nitrate ion. Furthermore, the spectrum exhibits bands [8] characteristic of structural OH^- (at 3640 cm^{-1}). Additionally, it also displays absorptions at 1035, 1460, 1310 and 745 cm^{-1} which are assigned to $Ni(NO_3)_2 \cdot 4H_2O$. In contrast, XRD of the calcination product at 220°C (Fig. 4) exhibits a pattern which contains the lines characteristic of

$Ni(NO_3)_2 \cdot 2H_2O$ (ASTM card no. 24-796) as well as those for $Ni(NO_3)_2 \cdot 2Ni(OH)_2$ (ASTM card no. 22-752).

The non-isothermal kinetic activation energy calculated for stage IV amounts to 130 kJ mol^{-1}. This value is higher than that expected for the tetra → dihydrate transformation.

In terms of these results, one must conclude that heating NiNHH to 220°C gives rise to the formation of a mixture of dihydrate and the basic nickel nitrate intermediates. Such compounds have been detected. [3, 10, 11].

The formation of the basic nitrate during the decomposition of NiNHH in static air [12] was attributed to hydrolysis of the nitrate by water vapour. In the present study, under dynamic atmosphere of air, water vapour is not available. Hence it could be presumed that water present within the nitrate was responsible for the hydrolysis process which leads to the formation of the basic nitrate intermediate under dynamic atmosphere of air.

Stage V

On raising the temperature, the TG curve (Fig. 1) indicates that the weight loss continued at a slower rate up to 240°C, where an accelerated and marked weight loss process occurred up to 255°C giving rise to a relatively stable material in the temperature range 260–300°C. The total weight loss corresponding to this event amounts to 46% of the original weight. The DTA curve indicates that this event is sharp and endothermic in nature.

The IR spectrum obtained for the calcination product at 270°C (Fig. 3, curve d) displays the bands characteristic of $Ni(NO_3)_2$ (1033, 1383 cm^{-1}) [8]. The spectrum also reveals the disappearance of the characteristic bands of the basic nitrate. Furthermore, absorptions at 640, 450 and 320 cm^{-1} are also present and these are assigned to NiO [13].

From the above results, the weight loss processes observed up to 255°C can be correlated with a partial decomposition of $Ni(OH)_2$ of the basic nickel nitrate to $NiO \cdot xH_2O$ in addition to the dehydration of the dihydrate intermediate.

It is worth mentioning that, in an earlier study [14], the decomposition of $Ni(OH)_2$ prepared from $Ni(NO_3)_2 \cdot 6H_2O$ at 300°C and 400°C gave rise to $NiO \cdot 0.5H_2O$ at both temperatures. XRD of the calcination product at 270°C, shown herein (Fig. 4), displays ill-defined characteristic lines of NiO (ASTM card no. 22-1189) in addition to those of the nitrate. Hence, one could presume that the intermediate obtained at 260–300°C has the composition $xNi(NO_3)_2 \cdot y(NiO \cdot 0.5H_2O)$. Such a composition explains the presence of absorptions due to H_2O in the IR spectrum. It is to be noted from Fig. 1 that the total weight loss up to the formation of this intermediate (stage V) increases with increasing the heating rate. This may infer that the hydrolysis process involving the water present within the nitrate is favoured at higher heating rate.

Stage VI

This final endothermic event extends over the temperature range 310–350°C (DTA curve, Fig. 1) and brings the total loss up to 72% of the original weight (TG, Fig. 1). The weight loss accompanying this process could be due to the decomposition of nickel nitrate. The non-isothermal activation energy for this event amounts to 94 kJ mol^{-1}. However the IR spectrum of the calcination product at 350°C (Fig. 3, curve e) exhibits the characteristic absorptions of water; this reveals that this product still retains a portion of $NiO \cdot 0.5H_2O$ which, as stated earlier [14, 15], is thermally stable up to 400°C.

It is to be noted from TG results (Fig. 1) that the loss of weight continues up to 420°C bringing the total loss up to 73% of the original weight. Furthermore, the IR spectrum of the calcination product at 400°C (Fig. 3, curve f) still exhibits the characteristic absorptions of NO_3^- ion and water of low intensity. The NO_3^- ion is hardly detectable in the spectrum of the calcination product at 600°C (Fig. 3, curve g). However, absorptions due to water are displayed, which agrees with an earlier study [14], where calcination of $Ni(OH)_2$ up to 700°C gave rise to the composition $NiO \cdot xH_2O$ (where x is in the range 0.7–0.1). It is worth noting that XRD analyses of the calcination products at 350, 400 and 600°C (Fig. 4) reveal the formation of NiO (ASTM card no. 22-1189) in the temperature range above 350°C.

THERMAL DECOMPOSITION UNDER NITROGEN ATMOSPHERE

Figure 5 shows the thermal behaviour of NiNHH under a dynamic atmosphere of nitrogen (30 cm^3 min^{-1}) and at heating rate of 10 K min^{-1}. TG and DTA curves under the same conditions, but using dynamic atmosphere of air, are shown below for comparison. The figure reveals that the thermal decomposition of NiNHH under nitrogen atmosphere occurs at lower temperatures than under air atmosphere. Moreover, DTA under nitrogen atmosphere shows that the decomposition of NiNHH proceeds through only five events, instead of six in air. The DTA curve obtained in nitrogen traces all the thermal events of NiNHH encountered in air except stage III which corresponds to the formation of the tetrahydrate intermediate. This may imply that the formation of such an intermediate in nitrogen flow is not favoured or it may decompose instantaneously after its formation.

It is interesting to note that in a dynamic nitrogen atmosphere, the formation of the basic nitrate intermediate occurs at lower temperature than in air. It has been stated elsewhere [3] that, the presence of 2 Torr of water vapour during the decomposition of NiNHH did not lead to the

formation of the basic nitrate intermediate. The absence of such an intermediate was attributed to the lower pressure of H_2O than that needed for the hydrolysis process. However, it seems that this is not the case, since the formation of that basic intermediate was observed under nitrogen flow which pre-empts the absence of water vapour. This in turn supports the conclusion that the formation of basic nickel nitrate occurs through a hydrolysis process involving the water of the dihydrate intermediate.

It is to be noted that at 450°C the TG curve in nitrogen indicates that the decomposition of NiNHH was completed with no further weight loss at higher temperatures. This may suggest that the final decomposition product under a nitrogen atmosphere is composed only of NiO with no water content in the temperature range above 450°C.

Finally, the following conclusions can be drawn:

(1) The thermal decomposition of nickel nitrate hexahydrate to produce NiO under dynamic atmosphere of air includes the following pathways

$$Ni(NO_3)_2 \cdot 6H_2O \text{ (solid)} \xrightarrow{I} Ni(NO_3)_2 \cdot 6H_2O \text{ (melt)} \xrightarrow{II}$$

$$(Ni(NO_3)_2) \cdot 5.5H_2O \rightleftharpoons 0.5[Ni_2(H_2O)_{11}(NO_3)_4] \xrightarrow{III}$$

$$Ni(NO_3)_2 \cdot 4H_2O \xrightarrow{IV}$$

$$Ni(NO_3)_2 \cdot 2H_2O + 2Ni(NO_3)_2 \cdot Ni(OH)_2 \xrightarrow{V}$$

$$xNi(NO_3)_2 \cdot y(NiO \cdot 0.5H_2O) \xrightarrow{VI} NiO \cdot nH_2O \xrightarrow{\Delta} NiO$$

(2) Basic nickel nitrate was identified as an intermediate throughout the thermal decomposition of NiNHH even under nitrogen atmosphere.

Scanning electron microscopy

SEM studies of the parent NiNHH revealed a narrow distribution in the size of well formed crystals with flat surfaces (Fig. 6(a, b)).

Scanning electron photomicrographs taken for sample heated at 270°C show considerable phenomenological changes compared to the unreacted NiNHH as seen in Fig. 7(a–c). Fig. 7(a) shows a froth-like structure. An obvious feature of such structure is the presence of rounded holes (Fig. 7(b)). Such structure appeared in all the crystal faces as clear in Fig. 7(c). It has been reported [16] that the development of the froth-like structure requires some reactant mobility indicating that the initial, and more rapid, first stage of the reaction is accompanied by melting, probably local and temporary, and the decomposition occurs within the molten phase. This is in accord with the results where the earlier endothermic event was attributed to a melting process accompanied by the release of $0.5H_2O$ (Fig.

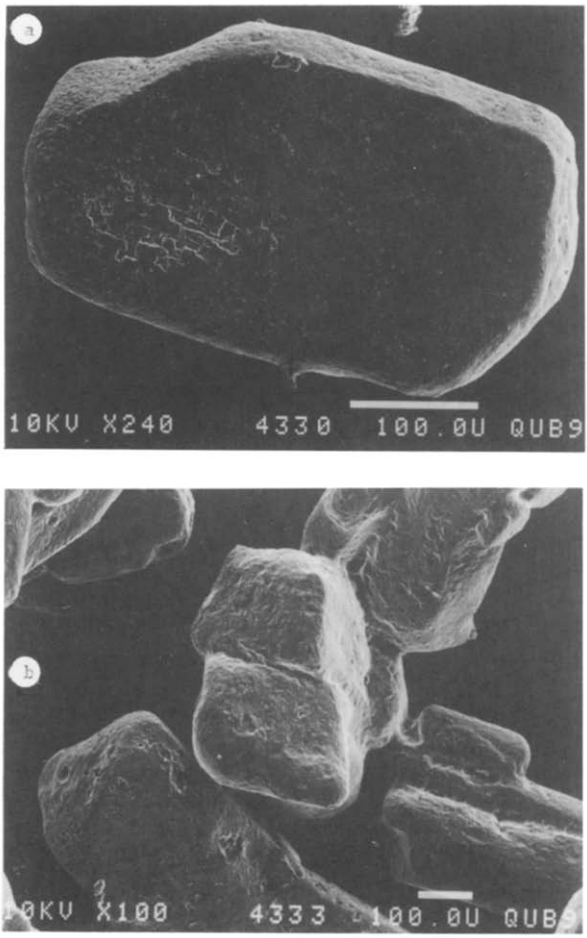

Fig. 6. Scanning electron micrographs of (a) the parent NiNHH showing flat surface crystals and (b) narrow size distribution.

1). Hence the release of such a low amount of water from the molten phase caused the appearance of the rounded holes in Fig. 7(c).

The morphological features observed at 270°C were exaggerated at 400°C. The froth-like structure was maintained with relatively smaller particle size (Fig. 8(a)). A typical fractured surface of NiNHH at 400°C is seen in Fig. 8(b). The surface showed cavities with curved edges indicating that they were originally bubbles. The variation in sizes and the distortions from spherical shape of the cavities were ascribed to irregular coalescence of gas pockets during growth within a medium of locally variable composition and viscosity. It is worth noting that the original crystal turned into an agglomerate which makes it clear that the decomposition process is accompanied by cracking of these grains (Fig. 8(c)).

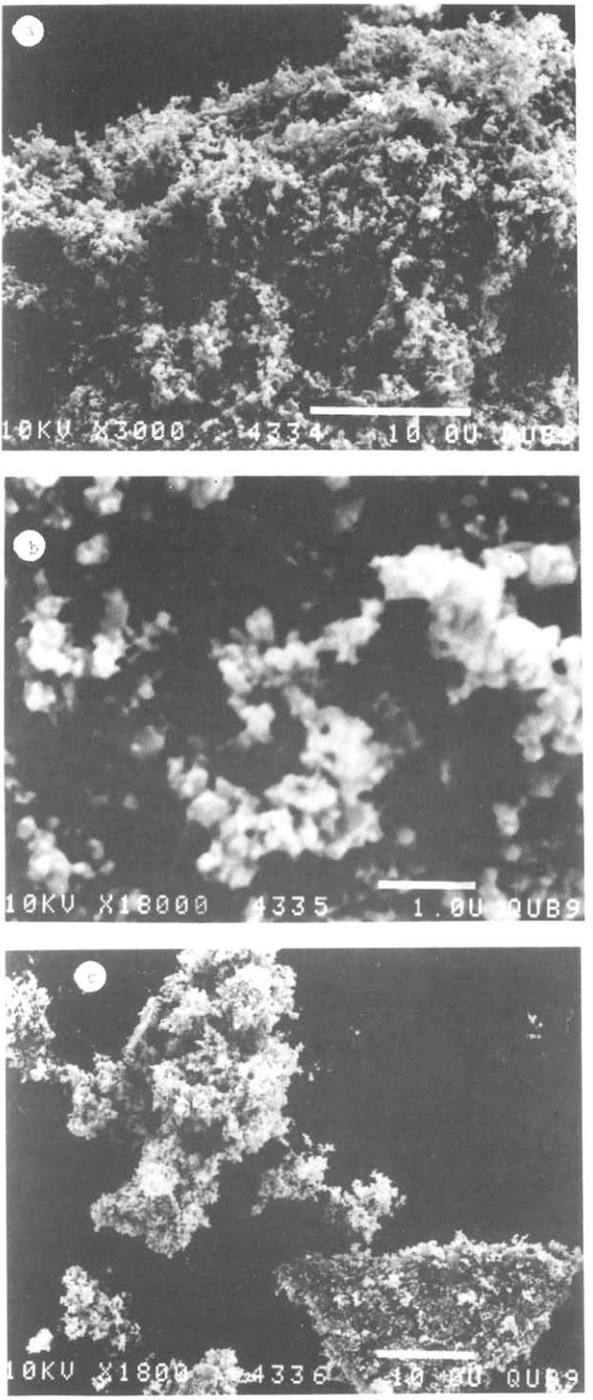

Fig. 7. Scanning electron micrographs of the decomposition product at 270°C revealing (froth-like structure (b) with small rounded holes, which (c) appeared in all the crystal fa

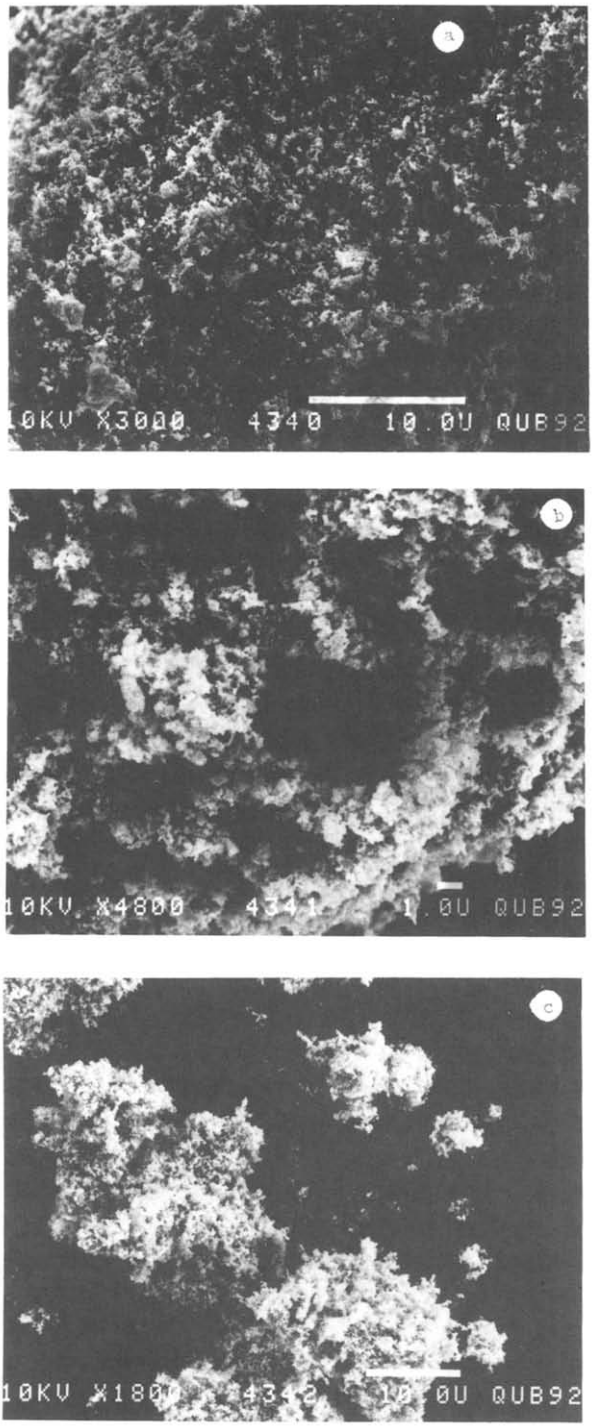

Fig. 8. Scanning electron micrographs of the calcination product at 400°C exhibiting (a, b) a froth-like structure with smaller particles and (c) the surface with cavities having curved edges.

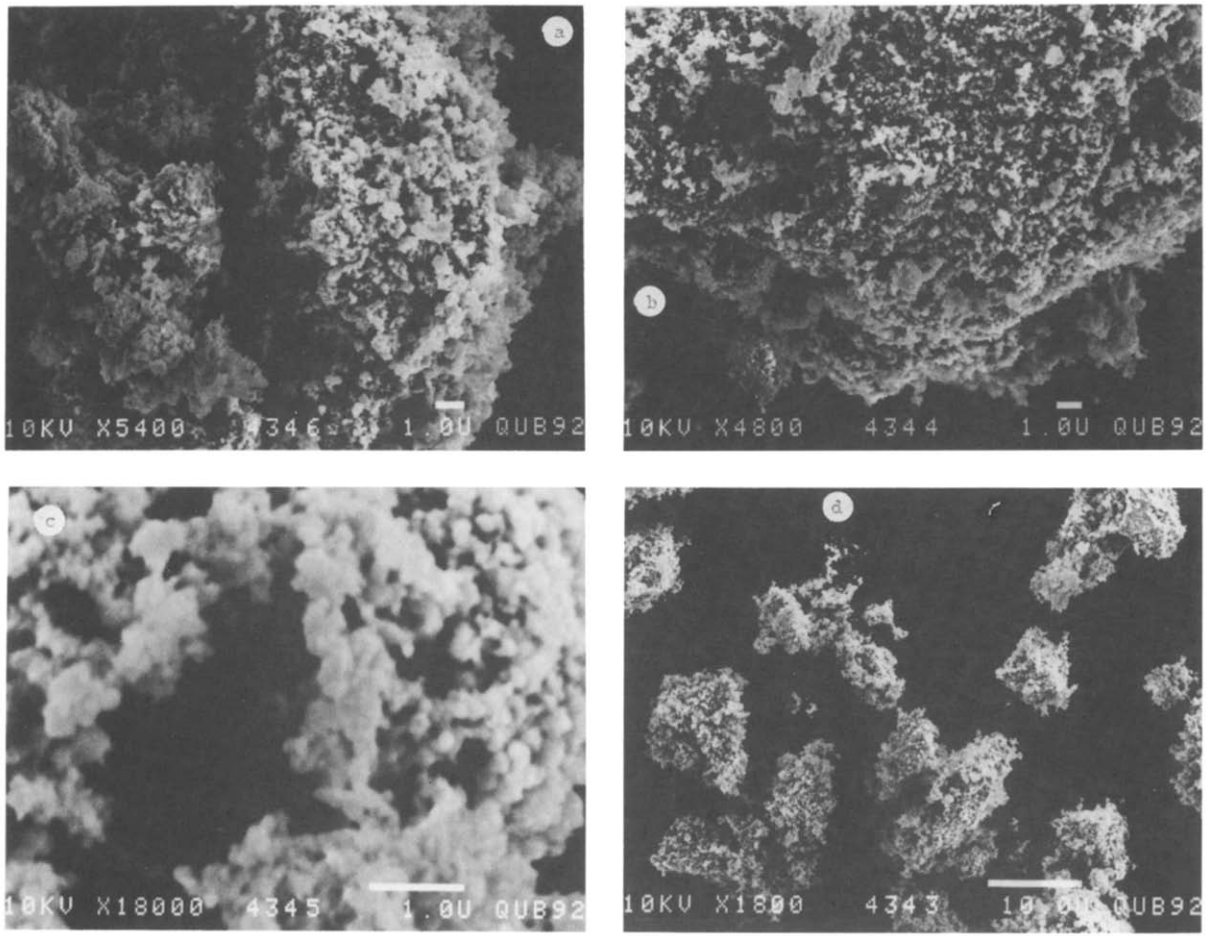

Fig. 9. Scanning electron micrographs of the final decomposition product showing (a) cracks on the surface, (b) grain edges, (c) non-spherical holes on the surface and (d) aggregates of the formed NiO.

Examination of the product obtained at 600°C (Fig. 9(a)) supported the suggestion that the decomposition was accompanied by cracks. Grain edges (Fig. 9(b)) revealed the permanence of such cracks where the grains appeared layered. The formation of these cracks was accompanied by an increase in the departure from spherical shape of the pores, as seen in Fig. 9(c). Figure 9(d) shows a collection of the decomposition product of NiNHH at 600°C which appeared as composite of froth-like layers apparently formed from aggregates of fine NiO crystallites.

These observations summarized the successive morphological changes accompanying the thermal decomposition of NiNHH which are in good accord with the physicochemical results.

ACKNOWLEDGEMENTS

It is a pleasure to thank the Queen's University of Belfast, particularly the staff of the Electron Microscope Unit, for assistance in obtaining the electron micrographs. Thanks are also due to the Egyptian Government for the grant of a Fellowship.

REFERENCES

1 W.W. Wendlandt, Thermochim. Acta, 10 (1974) 101.
2 J. Mu and D.D. Perlmutter, Thermochim. Acta, 56 (1982) 253.
3 D. Dollimore, G.A. Gamlen and T.J. Taylor, Thermochim. Acta, 86 (1985) 119.
4 D. Dollimore, G.A. Gamlen and T.J. Taylor, Thermochim. Acta, 91 (1985) 287.
5 J.M. Criado, A. Ortega and C. Real, React. Solids, 4 (1987) 93.
6 T. Ozawa, J. Therm. Anal., 2 (1970) 301.
7 A.W. Coats and J.P. Redfern, Nature (London), 201 (1964) 68.
8 J.A. Gadsden, Infrared Spectra of Minerals and Related Inorganic Compounds, Butterworths, London, 1975. pp. 15, 16.
9 S.D. Ross, Inorganic Infrared and Raman Spectra, McGraw-Hill, Maidenhead, UK, 1972, pp. 150–157.
10 J. Grant (Ed.), Hack's Chemical Dictionary, McGraw-Hill, New York, 1969, p. 478.
11 D. Weigal, B. Imelik and P. Laffitte, Bull. Soc. Chim. Fr., (1962) 345.
12 D. Weigal, B. Imelik and M. Prettre, C.R. Acad. Sci., 14 (1964) 2215.
13 F.F. Bently, L.D. Smithson and A.L. Rozek, Infrared Spectra and Characteristic Frequences ≈700–300 cm^{-1}, Wiley, New York, 1968, p. 1540.
14 M.I. Zaki, S.A.A. Mansour and R.B. Fahim, Surf. Technol., 25 (1985) 287.
15 W.M. Keely and H.W. Maynov, J. Chem. Eng. Data, 8 (1963) 297.
16 N.J. Carr and A.K. Galwey, Proc. R. Soc. London, Ser. A, 404 (1986) 101.